Cellular and Molecular Neurobiology (2019) 39:1125–1137
https://doi.org/10.1007/s10571-019-00707-2

ORIGINAL RESEARCH

CeO_2@PAA-LXW7 Attenuates LPS-Induced Inflammation in BV2 Microglia

Jingjing Jia[1,2] · Changyan Li[3] · Ting Zhang[4] · Jingjing Sun[2] · Sijia Peng[2] · Qizhi Xie[2] · Yining Huang[1] · Li Yi[2]

Received: 20 February 2019 / Accepted: 13 June 2019 / Published online: 29 June 2019

Abstract

Microglia are the inherent immune effector cells in the central nervous system (CNS), are activated rapidly when the CNS is stimulated by ischaemia, infection, injury, etc. and participate in and aggravate the development of inflammatory reactions in the CNS. During the process of microglial activation, inflammatory factors such as TNF-α and IL-1β and an abundance of reactive oxygen species (ROS)/reactive nitrogen species (RNS), are released by damaged nerve cells. LXW7 is a small molecule peptide and specifically binds with integrin αvβ3. Cerium oxide nanoparticles (nanoceria) are strong free radical scavengers and are widely used in many studies. In this research, a model of inflammation was established using lipopolysaccharide (LPS) to induce BV2 microglia activation, and the effects of CeO_2@PAA (synthetic nanoscale cerium oxide particles), LXW7 and CeO_2@PAA-LXW7 were evaluated. We detected the expression level of inflammatory factors, the release of NO in BV2 cells and the generation of intracellular ROS. The expression levels of focal adhesion kinase (FAK) and signal transducer and activator of transcription 3 (STAT3) and their phosphorylated proteins were detected in BV2 microglia. We found that CeO_2@PAA, LXW7 and CeO_2@PAA-LXW7 all effectively inhibited the activation of BV2 microglia, reduced the production of cytokines and the release of NO and reduced the production of intracellular ROS. The three treatments all inhibited the phosphorylation of FAK and STAT3 in BV2 microglia. Regarding these effects, CeO_2@PAA-LXW7 was more effective than the other two monotherapies. Our data indicate that CeO_2@PAA, LXW7 and CeO_2@PAA-LXW7 can exert a neuroprotective function by inhibiting the inflammatory response of LPS-induced BV2 microglia. LXW7 may inhibit the activation of FAK and STAT3 signals in combination with integrin αvβ3 to restrain neuroinflammation and the antioxidative stress effect of cerium oxide; hence, CeO_2@PAA-LXW7 can exert a more robust anti-inflammatory and neuroprotective effect via synergistically suppressing the ability of LXW7 to influence the integrin pathway and the free radical-scavenging ability of CeO_2@PAA.

Keywords Cerium nanoparticles · LXW7 · Integrin αvβ3 · Inflammation · Oxidative stress

✉ Yining Huang
ynhuang@bjmu.edu.cn

✉ Li Yi
yilitj@hotmail.com

Jingjing Jia
jiajingjing1005@bjmu.edu.cn

Changyan Li
celicy@imu.edu.cn

Ting Zhang
crystalting@foxmail.com

Jingjing Sun
sjingtemo@163.com

Sijia Peng
psj@bjmu.edu.cn

Qizhi Xie
407990339@qq.com

[1] Department of Neurology, Peking University First Hospital, No.8 Xishiku Street, Xicheng District, Beijing 100034, China

[2] Department of Neurology, Peking University Shenzhen Hospital, Shenzhen 518036, Guangdong Province, China

[3] College of Chemistry and Chemical Engineering, Inner Mongolia University, Hohhot, Inner Mongolia Province, China

[4] Department of Phoenix International Medical Center, The Fifth Affiliated Hospital of Sun Yat-sen University, Zhuhai, Guangdong Province, China

Introduction

Microglia are the innate immune cells of the central nervous system (CNS) and are one of the most important cellular components that induce the neuroinflammatory response. Under physiological conditions, microglia exhibit a multibranched, long convex shape. By constantly stretching and contracting their protrusions protuberances, microglia interact with neurons, astrocytes and blood vessels to monitor the CNS and synapses to detect tissue damage and pathogen infection. Microglial activation is a fundamental response to almost all CNS damage, including neurodegenerative diseases, local or systemic infections, cerebral ischaemia and trauma. Microglia can respond rapidly to the pathological stimulation of the CNS, become activated and undergo an obvious morphological change from branch-shaped cells to round, amoeba-shaped cells with short protrusions and phagocytic activity (Liddelow et al. 2017).

When the CNS is damaged, microglia can become activated and proliferate to remove tissue metabolites, apoptotic cells, damaged tissue and cell debris and help repair the damaged nervous system. However, continuously activated microglia secrete a large number of inflammatory mediators, such as TNF-α and IL-1β, reactive oxygen species (ROS) and reactive nitrogen species (RNS), etc., thus impairing mitochondrial function, leading to neuronal degeneration and necrosis, and further aggravating CNS damage (Thameem Dheen et al. 2007). Activated microglia can be induced by various stimuli, such as lipopolysaccharide (LPS), leading to the release of inflammatory cytokines, chemokines and ROS/RNS, which essentially cause neurotoxic reactions.

Integrins, which are cell adhesion molecules, are transmembrane glycoproteins that are widely found in cells. Integrins mediate the interaction of cells with the extracellular matrix, recognize and bind to corresponding ligands in the extracellular matrix as cell surface receptors and participate in the regulation of cell movement, proliferation and apoptosis. In addition, they can mediate synaptic reorganization and regulation and receptor localization in dendritic neurons (Cabodi et al. 1999; Goodman and Picard 2012; Kerrisk and Koleske 2013; Scheiffele et al. 2000). Many pathological processes, such as inflammation, thrombosis, invasion and metastasis, are associated with the abnormal regulation of integrins (Becchetti and Arcangeli 2010). Many previous studies have shown that many integrins (including αv and β1, β3, β5 and β8) localize to the postsynaptic regions of hippocampal neurons (Chan et al. 2003, 2006; Kramar et al. 2003; Mazalouskas et al. 2015; Nishimura et al. 1998; Pozo et al. 2012).

Integrin αvβ3 is a vitronectin receptor that is bidirectionally linked to the extracellular matrix (ECM) and intracellular signal transduction pathways (Hynes 2002). The binding of integrin αvβ3 to its ligand depends on the ligand's unique Arg-Gly-Asp (RGD) sequence. The structure of cyclo-Arg-Gly-Asp-D-Phe-Val (cyclo-RGDfv) is similar to that of the RGD sequence, so it can specifically bind to αvβ3, thereby blocking its binding to the ligand and suppressing the signalling pathway in which integrin αvβ3 participates (Roland Haubner et al. 1996). Research by Mazalouskas has demonstrated that integrin αvβ3 is widely expressed in the synapses of nerve endings in different brain regions and plays a key role in the regulation of many receptor-triggered intracellular signal transduction pathways (Mazalouskas et al. 2015). Many studies have shown that anti-angiogenic and anti-tumour effects can be exerted by binding to integrin αvβ3 on vascular endothelial cells and tumour cells (Chen et al. 2012; Diao et al. 2012; Gao et al. 2015; Wu et al. 2013). Some studies have demonstrated that integrin-associated signalling pathways play a vital role in regulating the activity of antioxidant enzymes and are involved in H_2O_2-induced apoptosis and ROS production in multifarious cell types (Liu et al. 2016; Yasuda et al. 2017). Integrin αvβ3 is involved in inflammatory and apoptotic processes by regulating intercellular signalling. In addition, integrin αvβ3 regulates the function of mitochondrial and cellular activity via modulating the focal adhesion kinase (FAK) and signal transduction and activation of transcription 3 (STAT3) pathways (Visavadiya et al. 2016). The inhibition of integrin αvβ3 reduces FAK phosphorylation, which is associated with decreased ROS production, suggesting that the integrin-FAK pathway is involved in the regulation of ROS production in glioma cells (Xu et al. 2015).

Nano cerium oxide (CeO_2) is a new type of powerful free radical-scavenging drug that can overcome the shortcomings of former therapies for ischaemic damage. Many studies have shown that CeO_2 particles can potently resist oxidative stress, indicating that they have the protective effect of scavenging ROS. They can reversibly combine with oxygen and transition to a Ce^{4+} or Ce^{3+} state during the redox reaction, making them able to actively scavenge oxygen (Esch et al. 2005; Robinson et al. 2002). Many studies have shown that nano CeO_2 can strongly induce antioxidant stress. For example, Schubert et al. (2006) found that CeO_2 can protect hippocampal neurons against oxidative stress. Niu et al. (2007) found that CeO_2 can reduce the production of NO and peroxynitrite in a mouse model of myocardial ischaemia. In addition, Estevez's study found that nano CeO_2, as an effective treatment, can reduce oxidation and nitrification after stroke in the hippocampus of an ischaemic mouse model (Estevez et al. 2011). These studies demonstrate that nano CeO_2 protects the CNS via scavenging ROS and RNS.

LXW7 is a small cyclic peptide designed and synthesized using one-bead one-compound (OBOC) combinatorial

chemistry and high-efficiency screening technology. It can be specifically combined with integrin αvβ3 to hinder the binding of integrin αvβ3 to its ligands (Hao et al. 2017). LXW7 has a molecular structure similar to that of cyclo-RGDfv, which can bind to integrin αvβ3 and block pathways in which integrins are involved. Some studies have shown that LXW7 can attenuate the activation of microglia in rats with middle cerebral artery occlusion (MCAO), reduce the secretion of inflammatory factors and the infarct size and have a certain neuroprotective effect (Fang et al. 2016; Wang et al. 2016; Xiao et al. 2010). LXW7 is a small octameric peptide surrounded by a disulfide bond; it contains unnatural amino acids and is more resistant to proteolysis than linear peptides and peptides composed of natural amino acids. It has a built-in handle (a functional carboxyl) at the C-terminus that, through chemical bonds, can unite a variety of different functional substances, including specific drugs, imaging agents and nanomaterials (Xiao et al. 2010). Due to the special spatial structure of LXW7, it can bind to other small molecules such as nano CeO_2 without having an impact on its biological function (Xiao et al. 2010). We combined CeO_2@PAA, which formed from CeO_2 and PAA (polyacrylic acid), and biotinylated LXW7 to synthesize a novel biocomposite carrier (CeO_2@PAA-LXW7) by EDC (1-ethyl-3-(3-dimethylaminopropyl) carbodiimide) reaction. CeO_2@PAA and biotinylated LXW7 were combined after CeO_2 and PAA were synthesized by EDC reaction to synthesize a new type of biological composite carrier. CeO_2@PAA, which is more stable, is synthesized by modifying PAA functional groups on the surface of CeO_2. We previously found that CeO_2@PAA has a diameter of 2-5 nm by TEM, and XPS spectroscopy of Ce 3d showed many oxygen vacancies in CeO_2@PAA. The surface characteristics of CeO2@PAA-LXW7 were analysed by FT-IR spectroscopy. The peaks at 3500–2500 cm^{-1}, 1702 cm^{-1} and 2550 cm^{-1} illustrate O–H, C=O and –C=C– stretching vibration, and the bands at 1450 cm^{-1} and 1162 cm^{-1} represent the presence of COO– and C–O functional group (Jia et al. 2018).

Therefore, we investigated whether this complex can integrate the ability of LXW7 to block the integrin pathway and the ability of CeO_2@PAA to scavenge ROS for neuroprotection, as well as the molecular mechanisms that may be involved in these processes.

Methods

Preparation and Administration of Drugs

LXW7 is commercially available, and biotinylated LXW7, CeO_2@PAA and CeO_2@PAA-LXW7 were all provided by Dr. Changyan Li and her team at the Inner Mongolia University School of Chemical Engineering. The synthesis process was consistent with the method used in our previous studies (Jia et al. 2018). CeO_2@PAA, LXW7 and CeO_2@PAA-LXW7 were diluted to 100 μg/mL with PBS for use. The concentration of the drugs used in the experiment was determined by combining existing studies with our previous experimental results (Zhang et al. 2018).

Cell Culture and Treatment

Murine BV2 microglial cells were purchased from the Cell Resource Center, Peking Union Medical College. BV2 microglia were incubated in high-glucose Dulbecco's modified Eagle's medium (DMEM) (Gibco, China) with 10% (v/v) foetal bovine serum (FBS) (Gibco, America) and 1% penicillin–streptomycin in a humidified incubator at 37 °C with a 5% CO_2 atmosphere. BV2 microglia were seeded in 6-well plates at a density of 2×10^5 cells/well and cultured for 24 h for subsequent experiments. The BV2 microglia were treated with 1 mg/L LPS for 24 h to generate a model of inflammation. The cells were divided into (a) the control group, (b) the LPS alone group (1 mg/L LPS for 24 h), (c) the CeO_2@PAA + LPS group (1 μM CeO_2@PAA for 24 h followed by LPS for 24 h), (d) the LXW7 + LPS group (1 μM LXW7 for 24 h followed by LPS for 24 h) and (e) the CeO_2@PAA-LXW7 + LPS group (1 μM CeO_2@PAA-LXW7 for 24 h followed by LPS for 24 h).

Cell Viability Measurement

Cell viability was analysed using the cell counting kit-8 (Beyotime, China). BV2 cells were seeded in 96-well plates at the destiny of 1×10^6 cells/well. Then, 10 μL/well of CCK8 solution was added to each well, and the plates were incubated at 37 °C for 2–3 h. The number of viable cells was represented by the optical density (OD), which was measured using a multimode detector (Beckman Coulter, DTX880) at 450 nm. The OD value of the control group was set as 100% percent of cell viability.

Reverse Transcription and Real-Time PCR

Total RNA was extracted from BV2 microglia with TRIzol reagent (Takara, Japan) according to the manufacturer's instructions. cDNA was synthesized by reverse transcription using the PrimeScript™ RT reagent kit. Real-time PCR was performed with the LightCycler® 96 Real-Time PCR system (Roche Molecular Systems, USA) using SYBR® Premix Ex Taq™ II. The relative expression of the target gene was calculated using the $2^{-\Delta\Delta C_T}$ method. All PCR primers used are shown in Table 1.

Table 1 Primers used in this study

Gene	Forward primer (5′–3′)	Reverse primer (5′–3′)
TNF-α	CCCTCACACTCAGATCATCTTCT	GCTACGACGTGGGCTACAG
IL-1β	GCAACTGTTCCTGAACTCAACT	ATCTTTTGGGGTCCGTCAACT
iNOS	GTTCTCAGCCCAACAATACAAGA	GTGGACGGGTCGATGTCAC
β-actin	GGCTGTATTCCCCTCCATCG	CCAGTTGGTAACAATGCCATGT

Enzyme-Linked Immunosorbent Assay (ELISA)

The supernatant of BV2 microglia was collected after centrifugation. The TNF-α and IL-1β ELISA kit (R&D systems, MN, USA) was used to detect the secretion of TNF-α and IL-1β in the supernatant, and the specific steps were carried out according to the manufacturer's protocols. The absorbance at 450 nm of each well was measured with a multimode detector (Beckman Coulter, DTX880). According to the absorbance of the different concentration standards, the curve and equation of the measured cytokine content at the absorbance value were obtained. According to this equation, the content of the measured cytokines in each group was calculated. The equations for the measured cytokine content at the absorbance value were based on the instructions provided with the ELISA kit [TNF-α: $y = 440.91x - 20.248$, $R^2 = 0.99139$ and IL-1β: $y = 455.89x - 31.58$, $R^2 = 0.99407$ (y: cytokine content, pg/mL: x: absorbance value, OD)].

Immunofluorescence Staining

BV2 microglia were fixed with 4% paraformaldehyde in PBS and blocked in 5% bovine serum albumin (BSA) at room temperature. The cells were then exposed to a primary antibody overnight at 4 °C followed by incubation with Alexa Fluor 488 (Cell Signalling Technology, USA) for 30 min at room temperature. Images were captured using a fluorescence microscope (Leica DMi8).

Detection of Nitric Oxide (NO) Contents

The supernatant of BV2 microglia was collected after centrifugation and the NO concentration was detected using the Griess reagent (Beyotime Biotechnology, China) for 10 min at room temperature. The production of NO was evaluated by measuring the absorbance at 540 nm using a microplate reader. All experiments were performed in triplicate.

Measurement of ROS

Intracellular ROS levels were detected by 2,7-dichlorofluorescein diacetate (DCFH-DA). The cells were incubated in 10 μmol/L DCFH-DA for 30 min at 37 °C in the dark. The intracellular ROS levels were represented by the fluorescence intensities determined by the flow cytometer (BD Accuri C6 Plus).

Immunoblot Analysis

Protein samples were extracted from BV2 microglia using RIPA buffer and were measured with a BCA kit. The protein was isolated on SDS-PAGE gels and transferred onto polyvinylidene difluoride (PVDF) membranes, and then the membranes were blocked with 5% non-fat milk in Tris-Buffered saline with Tween-20 (TBST) buffer for 1 h. Then, the PVDF membranes were incubated with primary antibodies against FAK (1:1000, CST), pY397-FAK (1:500, CST), STAT3 (1:1000, CST), pS727-STAT3 (1:400, CST) and β-actin (1:1000, Abcam) at 4 °C overnight. Then, the cells were incubated with a secondary antibody (1:1000, CST) for 1 h at room temperature. The blots were developed using the enhanced chemiluminescence (ECL) detection system (Tanon 5220S). β-actin was used to confirm a comparable amount of protein in each lane.

Statistical Analysis

Statistical analysis was performed using SPSS 21.0 statistical software. All data are from three independent experiments. The measurement data are expressed as the mean ± standard deviation ($X \pm SD$). T test was used for comparisons between two groups, and one-way ANOVA followed by the SNK post hoc test was used for multiple groups. $p < 0.05$ was defined as a significant difference.

Results

Effects of CeO_2@PAA, LXW7 and CeO_2@PAA–LXW7 on the Viability of BV2 Microglia

It is apparent from Fig. 1 that very few differences exist between all groups. There was no significant effect of LPS on the viability of BV2 microglia. We also detected the effect of CeO_2@PAA, LXW7 and CeO_2@PAA-LXW7 on BV2 microglia. These results suggest that CeO_2@PAA, LXW7 and CeO_2@PAA-LXW7 exhibit little cytotoxicity on BV2 microglia.

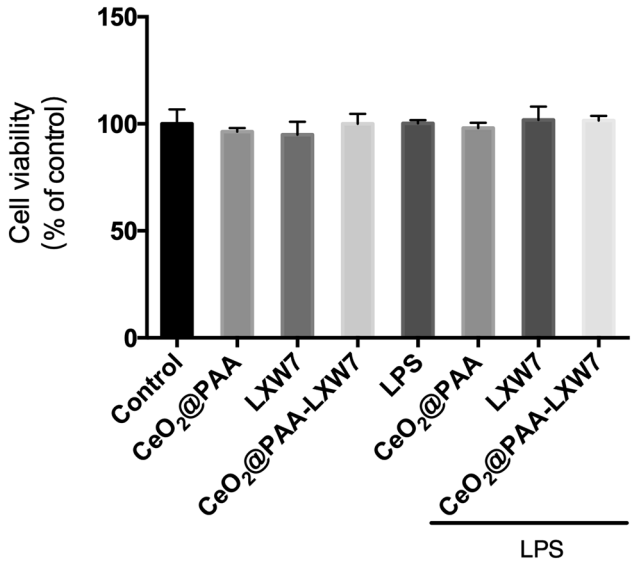

Fig. 1 The viability of BV2 microglia in each group after LPS treatment for 24 h. BV2 microglia were pre-incubated with CeO_2@PAA, LXW7 and CeO_2@PAA-LXW7 for 24 h, LPS was added for 24 h and the viability of the BV2 microglia was detected by the CCK8 kit

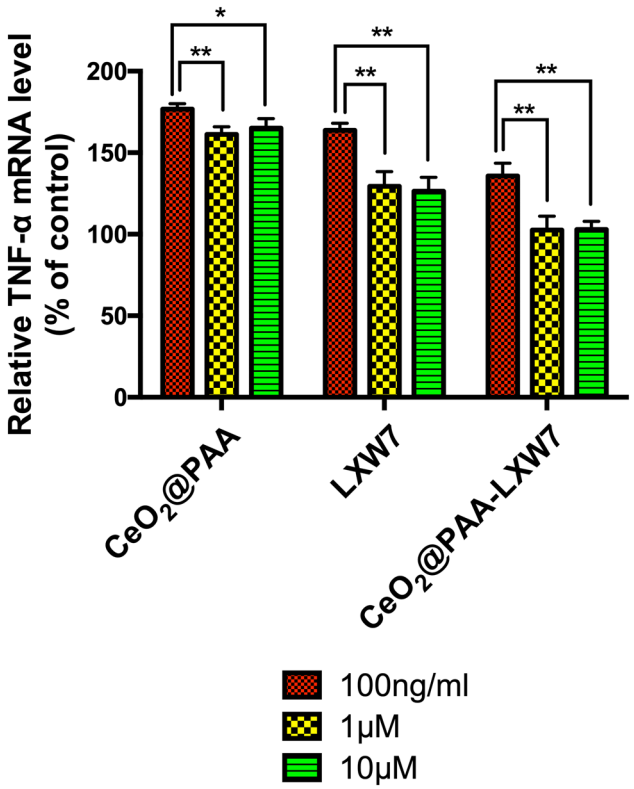

Fig. 2 The mRNA expression of TNF-α in BV microglia pretreated with CeO_2@PAA, LXW7 and CeO_2@PAA-LXW7 at concentrations of 100 ng/mL, 1 μM and 10 μM and activated by LPS (*$p<0.05$, **$p<0.01$)

Determination of Experimental Drug Concentration

We used qPCR to detect the effects of different concentrations of drugs on TNF-α mRNA expression and to compare the different effects of concentrations of 100 ng/mL, 1 μM and 10 μM. In the three administration groups, the 1 μM and 10 μM concentrations inhibited TNF-α more strongly than the 100 ng/mL concentration, while the effects of 1 μM and 10 μM did not differ significantly (Fig. 2).

Expression Levels of TNF-α and IL-1β in BV2 Microglia

As illustrated in Fig. 3a, the mRNA expression levels of TNF-α and IL-1β in the LPS-activated BV2 microglia were significantly improved compared with those in the control group (**$p<0.01$, **$p<0.01$). The mRNA expression levels of TNF-α and IL-1β in the CeO_2@PAA, LXW7 and CeO_2@PAA-LXW7 groups were decreased to different degrees than those in the LPS-activated group. The decreased levels of mRNAs were increased in the CeO_2@PAA-LXW7 group compared to the CeO_2@PAA group (**$p<0.01$, **$p<0.01$) and LXW7 group (*$p<0.05$, **$p<0.01$), and the difference was statistically significant. There was no significant difference in the expression of mRNAs between the CeO_2 and LXW7 groups, except for that of TNF-α in the LXW7 group, which was slightly lower than that in the CeO_2 group (*$p<0.05$).

We used an ELISA kit to detect the release of TNF-α and IL-1β in the cell culture supernatant of LPS-activated BV2 microglia (Fig. 3b). The results show that the amount of TNF-α and IL-1β secreted in the culture supernatant of LPS-activated BV2 microglia increased more than that in the control group (***$p<0.001$), while there was a reduction in the increased level of TNF-α and IL-1β in the CeO_2@PAA, LXW7 and CeO_2@PAA-LXW7 groups. Compared with that in the CeO_2@PAA and LXW7 groups, the secretion of TNF-α (**$p<0.01$) and IL-1β (**$p<0.01$, *$p<0.05$) was reduced in the CeO_2@PAA-LXW7 group, and the difference was statistically significant. In addition, the mRNA expression of TNF-α and IL-1β in the CeO_2@PAA-LXW7 group was not significantly different from that in the control group. However, when we detected extracellular secreted inflammatory factors, we found that the secretion in the CeO_2@PAA-LXW7 group was higher than that in the control group.

The expression and localization of inflammatory factors in the cytoplasm of BV2 microglia were observed by immunofluorescence staining. The results were basically consistent with the results of qPCR and ELISA; the expression of inflammatory factors in the BV2 cells in the control group was very low, and TNF-α and IL-1β were significantly expressed in the cytoplasm of BV2 microglia after LPS activation. A decrease in the expression of

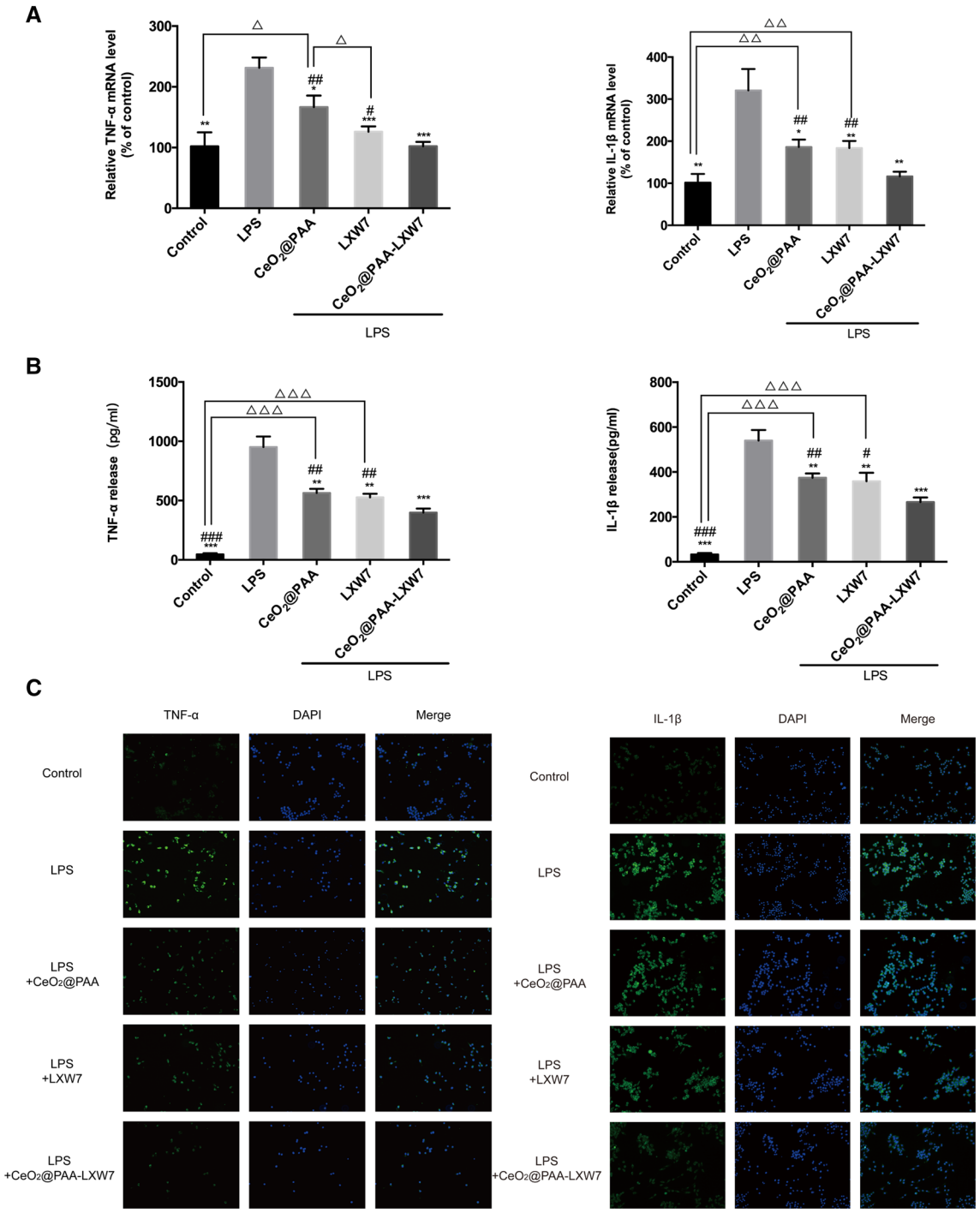

Fig. 3 The expression of TNF-α, IL-1β in LPS-activated BV2 microglia. **a** The relative mRNA expression of TNF-α and IL-1β in each group. **b** The secreted amount of TNF-α and IL-1β in the supernatant of BV2 microglia. **c** The expression of TNF-α and IL-1β in each group (green fluorescence; ×200 magnification) (*$p<0.05$, **$p<0.01$, ***$p<0.001$ compared with the LPS group; $^{\#}p<0.05$, $^{\#\#}p<0.01$ compared with the CeO_2@PAA-LXW7 group; the remaining differences are marked above the connecting line between the two groups, $^{\Delta}P<0.05$, $^{\Delta\Delta}P<0.01$, $^{\Delta\Delta\Delta}P<0.001$)

inflammatory factors was observed in the groups treated with CeO_2@PAA, LXW7 and CeO_2@PAA-LXW7, of which the CeO_2@PAA-LXW7 group exhibited the highest degree of reduction (Fig. 3c).

CeO_2@PAA-LXW7 Inhibits the Release of ROS and NO in BV2 Microglia Activated by LPS

The release of ROS and NO in BV2 microglia was detected

by the DCFH-DA fluorescence probe method and a NO test kit, respectively, and the iNOS mRNA level was detected by qPCR. As shown in Fig. 4, after LPS activation, the expression of iNOS mRNA and the secretion of NO and ROS were significantly increased (***$p<0.001$) in BV2 microglia, and CeO_2@PAA, LXW7 and CeO_2@PAA-LXW7 were able to reduce the production of ROS and NO to varying degrees. However, the administration of these treatments did not diminish the levels of ROS and NO secretion in LPS-induced BV2 microglia to levels similar to those in the control group. The degree to which the levels were reduced in the CeO_2@PAA-LXW7 group was higher than that in the CeO_2@PAA (***$p<0.001$) and LXW7 (***$p<0.001$) groups, and the difference was statistically significant. In addition, the secretion of NO and ROS in the LXW7 group was slightly lower than that in the CeO_2 group (**$p<0.01$, *$p<0.05$).

CeO_2@PAA-LXW7 Inhibits Integrin αvβ3 in LPS-Activated BV2 Microglia

The expression of integrin αvβ3 in BV2 microglia was detected by immunofluorescence staining. As shown in Fig. 5, integrin αvβ3 expression was significantly enhanced by LPS activation compared with that in control BV2 microglia. Both LXW7 and CeO_2@PAA-LXW7 inhibited the expression of integrin αvβ3, while the CeO_2@PAA group did not differ significantly from the LPS group. LXW7 and CeO_2@PAA-LXW7 had similar inhibitory effects, but still induced a certain degree of enhancement compared to that in the control group.

CeO_2@PAA-LXW7 Inhibits the Phosphorylation of FAK and STAT3 in LPS-Activated BV2 Microglia

To explore the mechanism of CeO_2@PAA-LXW7, we tested the protein expression of FAK and STAT3 and their phosphorylated forms (p-FAK and p-STAT3) in BV2 microglia. As shown in Fig. 6, we found that the total protein

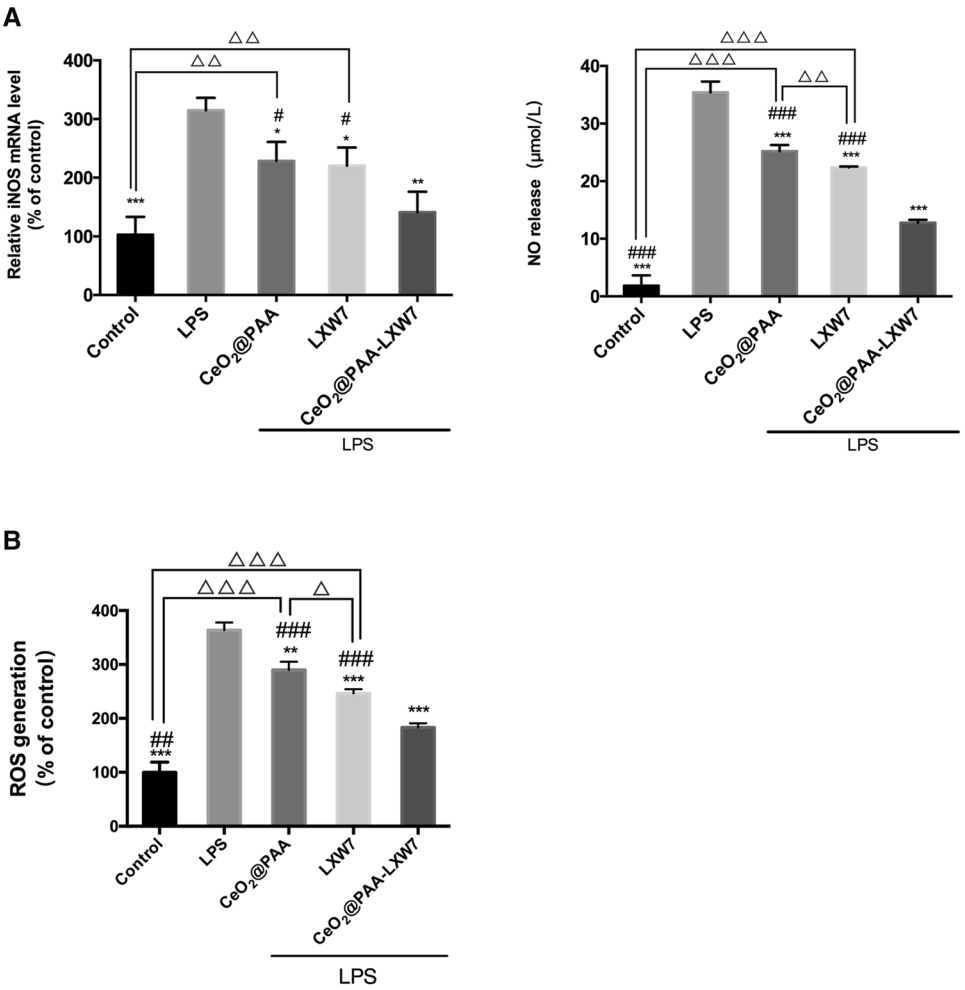

Fig. 4 The mRNA expression of iNOS and intracellular NO and ROS release from the culture supernatant of BV2 cells in each group 24 h after LPS induction. **a** The relative mRNA expression of iNOS and NO production. **b** Intracellular ROS production in the cell supernatant of each group (**$p<0.01$, ***$p<0.001$ compared with the LPS group, $^{\#\#\#}p<0.001$ compared with the CeO_2@PAA-LXW7 group; the remaining differences are marked above the connecting line between the two groups, $^{\Delta}P<0.05$, $^{\Delta\Delta}P<0.01$, $^{\Delta\Delta\Delta}P<0.001$)

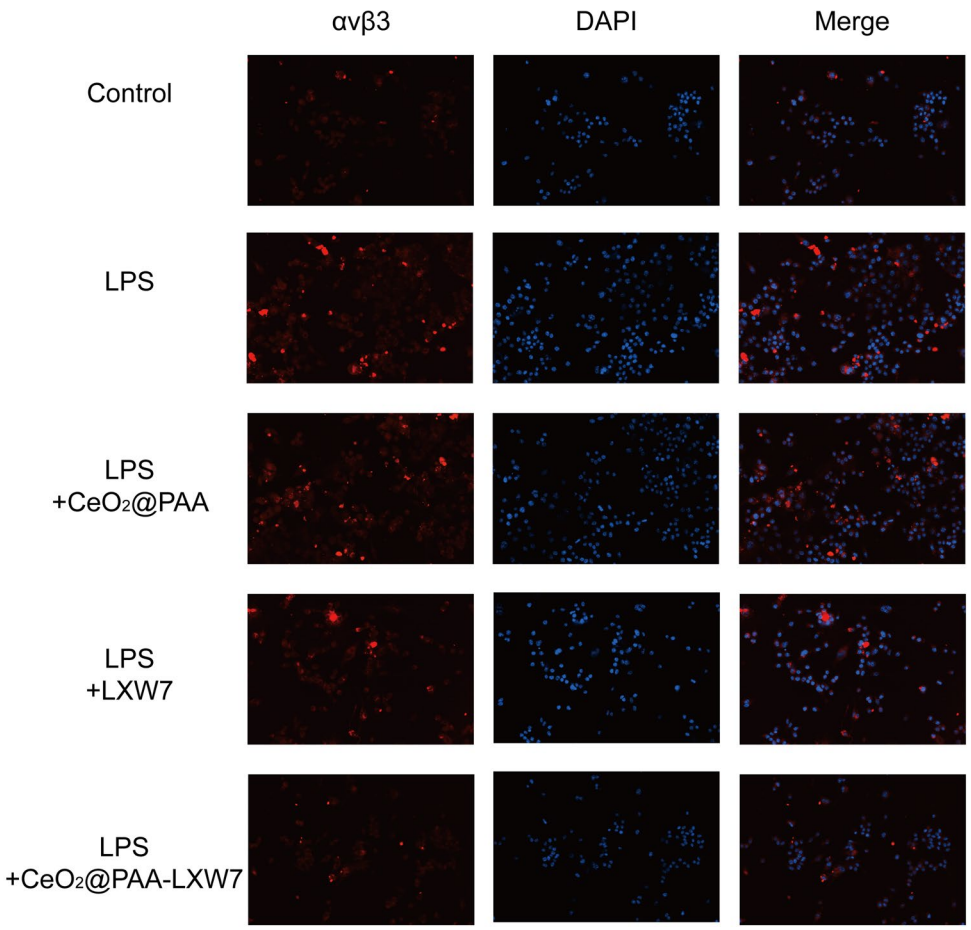

Fig. 5 Expression of integrin αvβ3 in LPS-activated BV2 microglia, as detected by fluorescence inverted microscopy. The expression of integrin αvβ3 in each group was displayed by red fluorescence (×200 magnification)

expression levels of FAK and STAT3 in each group were substantially unchanged, while the protein expression of p-FAK and p-STAT3, the activated forms, were significantly higher in the LPS-activated group than that in the control group. Both LXW7 and CeO_2@PAA-LXW7 were able to reduce the expression of p-FAK and p-STAT3. We also found that the phosphorylation level in the CeO_2@PAA group was lower than that in the LPS group, and the difference was significant.

Discussion

Many studies have found that the gene expression of inflammatory factors, such as TNF-α and IL-1β, is significantly upregulated within a few hours after cerebral ischaemia or hypoxic injury (Amantea et al. 2014; Tuttolomondo et al. 2014). TNF-α and IL-1β are very important pro-inflammatory factors that can directly induce the formation of many other inflammatory factors, further aggravating inflammation and increasing the number of toxic products in the CNS. Nitric oxide (NO) is an endogenous small molecule that acts as both a cellular messenger and a neurotransmitter, and it plays a wide-ranging role as a neurotransmitter in the CNS. Under the pathological conditions of inflammation after CNS injury, cells can produce a large amount of inducible nitric oxide (iNOS), which catalyses the production of NO by L-arginine. At present, it is through that, under pathological conditions in the CNS, reactive microglia overexpress iNOS to synthesize a large amount of the toxic free radical NO, which may be involved in apoptosis, mediate oxidative stress damage and cause neuronal damage (Jeon et al. 2014). Therefore, inhibiting the excessive activation of microglia and reducing the production of pro-inflammatory cytokines and toxic substances is the research focus of brain protection therapy.

We examined the mRNA expression of TNF-α in LPS-induced BV2 microglia after the administration of three different concentrations of drugs on, and we ultimately selected 1 μM as the experimental concentration. In our study, we also found that the expression levels of TNF-α, IL-1β and iNOS in BV2 microglia were significantly increased after LPS stimulation, and the secretion of TNF-α and IL-1β, ROS and NO also increased accordingly. Meanwhile, in the CeO_2@PAA, LXW7 and CeO_2@PAA-LXW7 pretreatment groups, the expression levels of these proteins were

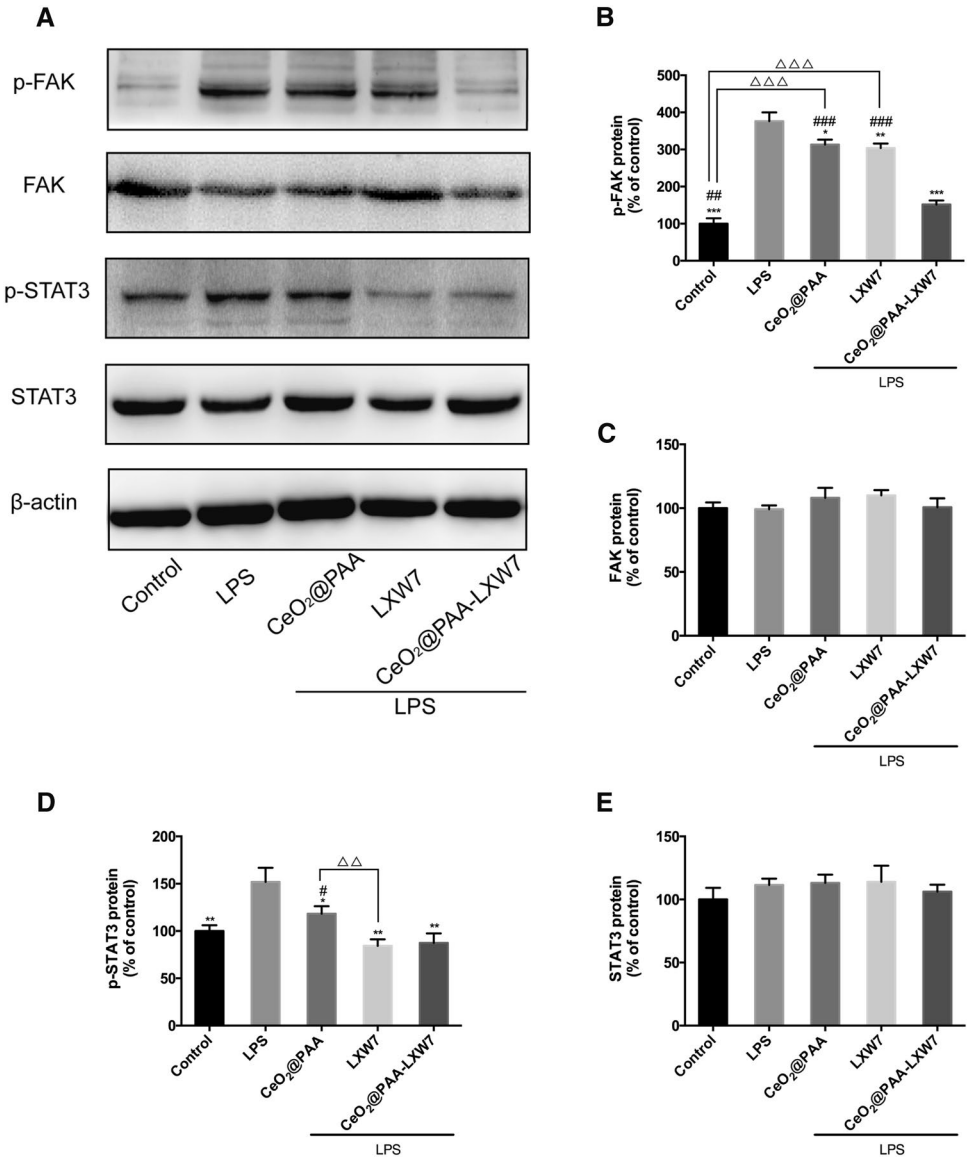

Fig. 6 Effects of CeO_2@PAA, LXW7 and CeO_2@PAA-LXW7 on the protein expression of p-FAK, FAK, p-STAT3, STAT3 in LPS-activated BV2 microglia. **a** Changes in the expression of p-FAK, FAK, p-STAT3, STAT3 in BV2 cells. **b–e** The results of the semi-quantitative analysis of protein greyscale ($^{*}p<0.05$, $^{**}p<0.01$, $^{***}p<0.001$ compared with the LPS group; $^{\#}p<0.05$, $^{\#\#}p<0.01$, $^{\#\#\#}p<0.001$ compared with the CeO_2@PAA-LXW7 group; the remaining differences are marked above the connecting line between the two groups, $^{\Delta\Delta}p<0.01$, $^{\Delta\Delta\Delta}p<0.001$)

decreased to different degrees compared with those in the control group, with the CeO_2@PAA-LXW7 group exhibiting the highest degree of decline and being significantly different from the other two groups. This indicates that CeO_2@PAA, LXW7 and CeO_2@PAA-LXW7 have anti-inflammatory effects, which can inhibit the activation of BV2 microglia to a certain extent, while the anti-inflammatory effect of CeO_2@PAA-LXW7 is stronger than that of the other two drugs.

Studies have shown that FAK expression is increased in a model of LPS-induced microglial activation, and because of the specificity of FAK and the fact that it is not expressed in immature astrocytes and oligodendrocyte lysates, it can be used as a potential target for inhibiting microglial activation (Krady et al. 2002). FAK can mediate the integrin pathway, is involved in the regulation of cell migration, proliferation and phagocytosis and is closely related to the activation of microglia (Chen and Guan 1996; Miranti et al. 1998; Takeuchi et al. 1997). Our study also found a significant increase in FAK phosphorylation in LPS-induced activated BV2 microglia.

The RGD sequence specifically binds to integrin αvβ3, blocks the integrin pathway and reduces FAK activation. The current study found that osteopontin (OPN), which contains the RGD sequence, binds to endogenous integrin αvβ3 in primary cultured microglia to inhibit iNOS expression and has neuroprotective and anti-inflammatory effects (Jin et al. 2015). Studies have shown that cyclic RGDfV can significantly attenuate the upregulation of activated microglia in the mouse brain after 1-methyl-4-phenyl-1,2,3,6 tetrahydropyridine (MPTP) injury, demonstrating that cyclic RGDfV has neuroprotective effects (Patel et al. 2011). Our study

used CeO_2@PAA-LXW7 to reduce the phosphorylation of FAK in LPS-induced BV2 microglia by blocking the integrin pathway via cyclic RGDfV. The phosphorylation of FAK is closely related to the inflammatory response of BV2 cells, which is consistent with the trend of inflammatory factors, ROS and NO release. CeO_2@PAA-LXW7 and LXW7 may inhibit the increase of the inflammatory response by inhibiting the excessive activation of FAK.

As an important immune signalling molecule, STAT3 is widely expressed in the CNS and plays an important role in regulating microglia activation and inflammatory responses (Dinapoli et al. 2010; Huang et al. 2008). STAT3 is an important factor in the regulation of inflammatory factor gene expression and a major indicator of CNS damage (Planas et al. 1996). Studies have shown that elevated levels of phosphorylated STAT3 expression are detected in activated microglia during cerebral ischaemic injury (Schäbitz et al. 2003). The activation of abnormally activated STAT3 is also involved in neuroinflammatory damage triggered by ischaemic stroke. Studies have found that STAT3 phosphorylation induced by focal ischaemia is localized to various cell types, including microglia, macrophages, astrocytes and neurons (Justicia et al. 2000; Planas et al. 1996; Suzuki et al. 2001). Our study also found that phosphorylated STAT3 expression is significantly increased after LPS-induced BV2 microglia, which is consistent with previous studies. CeO_2@PAA-LXW7 can significantly inhibit the increase of p-STAT3, inhibit the production of inflammatory factors and weaken the inflammatory response.

In recent years, many studies have shown that CeO_2 can freely shift between the trivalent state (Ce^{3+}) and the tetravalent state (Ce^{4+}), which enhances it antioxidant capacity and its ability to scavenge free radicals by sensitizing superoxide dismutase and catalase (Celardo et al. 2011; Clark et al. 2011; Li et al. 2014; Pirmohamed et al. 2010; Pourkhalili et al. 2011). Our findings are consistent with those of previous studies, which showed that the potential of CeO_2@PAA to decrease intracellular ROS and antioxidative stress damage. The LXW7 and CeO_2@PAA-LXW7 treatment groups also showed similar changes as those in the CeO_2@PAA treatment group. CeO_2@PAA formed after coating CeO_2 and PAA can react with LXW7 through EDC reaction to form the novel compound CeO_2@PAA-LXW7. We anticipate that CeO_2@PAA-LXW7 can synthesize LXW7 to block the integrin pathway and CeO_2@PAA to scavenge oxygen free radicals and exert neuroprotective effects on oxidative stress-induced apoptosis. According to our previous research, CeO_2@PAA-LXW7 can significantly diminish the infarct area and neuronal apoptosis and attenuate oxidative stress in MCAO rats (Zhang et al. 2018).

Integrin is widely expressed on a variety of cell surfaces and participates in various physiological processes, such as apoptosis, angiogenesis and cell migration. LXW7 (cGRGDdvc) is a small cyclic RGD peptide that specifically binds to integrin αvβ3 (Xiao et al. 2010). Some studies have demonstrated that LXW7 can reduce the infarct size in MCAO rats and attenuate the apoptosis of neurons (Fang et al. 2016; Wang et al. 2016; Xiao et al. 2010). Biotinylated LXW7 has a high affinity for integrin; in particular, it can bind to integrin αvβ3 to block its binding to ligands. Our study illustrated that the expression of αvβ3 in the LXW7- or CeO_2@PAA-LXW7-pretreated group was significantly lower than that in the LPS-activated BV2 microglia, demonstrating that LXW7 and CeO_2@PAA-LXW7 can inhibit the expression of αvβ3. Our previous studies have shown that CeO_2@PAA-LXW7 can reduce neuronal apoptosis by inhibiting the integrin pathway and the phosphorylation of FAK and STAT3, therefore exerting neuroprotective effects.

In summary, this study demonstrates that CeO_2@PAA, LXW7 and CeO_2@PAA-LXW7 have no significant cytotoxic effects against BV2 microglia and have no significant effect on cell viability. CeO_2@PAA, LXW7 and CeO_2@PAA-LXW7 all reduce the release of TNF-α and IL-1β from LPS-induced BV2 microglia, and both LXW7 and CeO_2@PAA-LXW7 significantly reduce p-FAK and p-STAT3 expression, with the latter being more powerful than the former. Based on these results, we hypothesize that CeO_2@PAA-LXW7 can suppress the phosphorylation of FAK and STAT3 by inhibiting the integrin pathway, thereby inhibiting the activation of microglia and the release of inflammatory factors, resulting in neuroprotective effects (Fig. 7). At the same time, we also found that CeO_2@PAA also reduces the expression of p-FAK and p-STAT3, and the degree of reduction in the CeO_2@PAA-LXW7 group was higher than that in the LXW7 group. This suggests that CeO_2 may also participate in the regulation of inflammation-related pathways, but the concrete mechanism needs further study.

In this study, we found that CeO_2@PAA-LXW7 can significantly inhibit LPS-induced BV2 microglia overactivation, reduce the release of inflammatory factors, ROS and RNS and attenuate the inflammatory response in BV2 cells, and its effect is stronger than that of CeO_2@PAA or LXW7 alone. By detecting FAK and STAT3 phosphorylation levels, we found that CeO_2@PAA-LXW7 significantly attenuates the phosphorylation of FAK and STAT3 in overactivated BV2 microglia, suggesting that CeO_2@PAA-LXW7 may suppress the inflammatory response by inhibiting FAK and STAT3 signalling. Our previous study found that the effects of the FAK and STAT3 pathways are also observed in PC12 cells. The activation of FAK and STAT3 promotes apoptosis in H_2O_2-induced PC12 cells, whereas CeO_2@PAA-LXW7 inhibits apoptosis by inhibiting the phosphorylation of FAK and STAT3(Jia et al. 2018). Combined with this study, we believe that FAK and STAT3 signalling is involved not only in the apoptosis of PC12 cells but also in the activation of BV2 microglia.

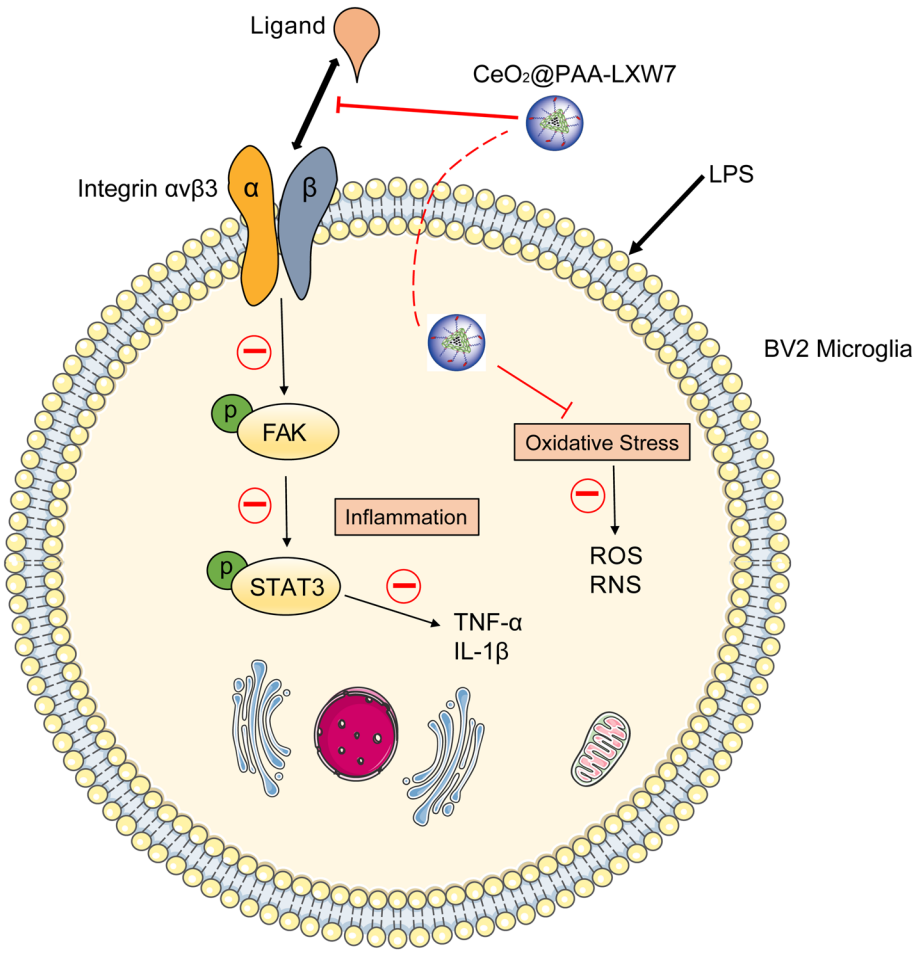

Fig. 7 Model of the mechanism by which CeO_2@PAA-LXW7 inhibits inflammation in BV2 microglia. LPS induces an inflammatory response to BV2 microglia, releases inflammatory factors and causes oxidative stress, which causes cells to release large amounts of ROS and RNS. CeO_2@PAA-LXW7 via inhibiting the binding of integrin αvβ3 to its ligand, sequentially suppresses the phosphorylation of FAK and STAT3, further prohibiting inflammatory responses. In addition, CeO_2@PAA-LXW7 also inhibits oxidative stress and reduces the production of ROS and RNS

CeO_2@PAA-LXW7 can inhibit the activation of integrin αvβ3 and the phosphorylation of FAK and STAT3. Therefore, we suspect that CeO_2@PAA-LXW7 can simultaneously resist neuronal apoptosis and microglial activation, which provides a theoretical basis for future research in vivo. Our findings provide a new and viable treatment for preventing further neurological damage following central nervous system injury. However, further research is needed to prove the safety, long-term effects and side effects of the drug.

There are some shortcomings of this study. We established the drug concentration through the literature and a preliminary experiment but did not refine the drug concentration. In the future, we should further study the effect of the drug concentration on neurological function and determine the best drug concentration. Our study found that CeO_2@PAA alone has a certain anti-inflammatory effect and has a certain inhibitory effect on the phosphorylation of FAK and STAT3, but we did not study the mechanism of action. Thus, it is necessary to further explore and study the specific mechanism. Integrins may be involved in a variety of signalling pathways in CNS diseases, and other important factors may be involved in the regulation of FAK and STAT3 signalling pathways. Further experimental research is needed in the future.

Author Contributions LY designed the study. CL synthesized the drugs. JJ, TZ and SP performed the studies. JS and QX assisted in part of the experiment. JJ analysed the data and wrote the paper. YH and LY edited the paper. All authors read and approved the final manuscript.

Funding This study was funded by the Basic Research Project of Peking University Shenzhen Hospital (JCYJ2018012), the Health and Family Planning Commission of Shenzhen Municipality Fund (SZSM201812096) and the Beijing Key Laboratory (BZ0250). The drug synthesis process was supported by the Inner Mongolia University Startup Fund Project (21300-5145152), the Inner Mongolia Education Department Key Project (NJZZ16015) and the Inner Mongolia Natural Science Foundation (2016MS0216).

Compliance with Ethical Standards

Conflict of interest The authors declare that they have no conflicts of interest.

Research Involving Human Participants and/or Animals This article does not contain any studies with human participants or animals performed by any of the authors.

References

Amantea D, Certo M, Russo R, Bagetta G, Corasaniti MT, Tassorelli C (2014) Early reperfusion injury is associated to MMP2 and IL-1β elevation in cortical neurons of rats subjected to middle cerebral artery occlusion. Neuroscience 277:755

Becchetti A, Arcangeli A (2010) Integrins and ion channels in cell migration: implications for neuronal development, wound healing and metastatic spread. Adv Exp Med Biol 674:107

Cabodi S et al (1999) Integrins and signal transduction. Curr Opin Hematol 6:37

Celardo I, Nicola MD, Mandoli C, Pedersen JZ, Traversa E, Ghibelli L (2011) Ce^{3+} ions determine redox-dependent anti-apoptotic effect of cerium oxide nanoparticles. ACS Nano 5:4537–4549

Chan CS, Weeber EJ, Kurup S, Sweatt JD, Davis RL (2003) Integrin requirement for hippocampal synaptic plasticity and spatial memory. J Neurosci 23:7107–7116 **The Official Journal of the Society for Neuroscience**

Chan CS, Weeber EJ, Zong L, Fuchs E, Sweatt JD, Davis RL (2006) β1-Integrins are required for hippocampal AMPA receptor-dependent synaptic transmission, synaptic plasticity, and working memory. J Neurosci 26:223 **The Official Journal of the Society for Neuroscience**

Chen HC, Guan JL (1996) The association of focal adhesion kinase with a 200-kDa protein that is tyrosine phosphorylated in response to platelet-derived growth factor. FEBS J 235:495–500

Chen WT, Shih TT, Chen RC, Tu SY, Hsieh WY, Yang PC (2012) Integrin αvβ3-targeted dynamic contrast-enhanced magnetic resonance imaging using a gadolinium-loaded polyethylene gycol-dendrimer-cyclic RGD conjugate to evaluate tumor angiogenesis and to assess early antiangiogenic treatment response in a mouse xenogr. Mol Imaging 11:286

Clark A, Zhu A, Sun K, Petty HR (2011) Cerium oxide and platinum nanoparticles protect cells from oxidant-mediated apoptosis. J Nanoparticle Res 13:5547–5555. https://doi.org/10.1007/s11051-011-0544-3

Diao Y et al (2012) Designed synthetic analogs of the α-helical peptide temporin-La with improved antitumor efficacies via charge modification and incorporation of the integrin αvβ3 homing domain. J Pept Sci 18:476–486 **An Official Publication of the European Peptide Society**

Dinapoli VA et al (2010) Age exaggerates proinflammatory cytokine signaling and truncates signal transducers and activators of transcription 3 signaling following ischemic stroke in the rat. Neuroscience 170:633–644

Esch F et al (2005) Chemistry: electron localization determines defect formation on ceria substrates. Science 309:752

Estevez AY et al (2011) Neuroprotective mechanisms of cerium oxide nanoparticles in a mouse hippocampal brain slice model of ischemia. Free Radic Biol Med 51:1155–1163. https://doi.org/10.1016/j.freeradbiomed.2011.06.006

Fang T, Zhou D, Lu L, Tong X, Wu J, Yi L (2016) LXW7 ameliorates focal cerebral ischemia injury and attenuates inflammatory responses in activated microglia in rats. Braz J Med Biol Res 49:e5287. https://doi.org/10.1590/1414-431X20165287

Gao Y et al (2015) Enhanced antitumor efficacy by cyclic RGDyK-conjugated and paclitaxel-loaded pH-responsive polymeric micelles. Acta Biomater 23:127–135

Goodman SL, Picard M (2012) Integrins as therapeutic targets. Trends Pharmacol Sci 33:405–412. https://doi.org/10.1016/j.tips.2012.04.002

Hao D et al (2017) Discovery and characterization of a potent and specific peptide ligand targeting endothelial progenitor cells and endothelial cells for tissue regeneration. ACS Chem Biol 12:1075–1086. https://doi.org/10.1021/acschembio.7b00118

Haubner R, Gratias R, Diefenbach B, Goodman SL, Jonczyk A, Kessler H (1996) Structural and functional aspects of RGD-containing cyclic pentapeptides as highly potent and selective integrin αvβ3 antagonists. J Am Chem Soc 118(32):7461–7472

Huang C, Ma R, Sun S, Wei G, Fang Y, Liu R, Li G (2008) JAK2-STAT3 signaling pathway mediates thrombin-induced pro-inflammatory actions of microglia in vitro. J Neuroimmunol 204:118

Hynes RO (2002) Integrins: bidirectional, allosteric signaling machines. Cell 110:673

Jeon CM et al (2014) Siegesbeckia glabrescens attenuates allergic airway inflammation in LPS-stimulated RAW 264.7 cells and OVA induced asthma murine model. Int Immunopharmacol 22:414

Jia J et al (2018) Neuroprotective effect of CeO_2 @PAA-LXW7 against H_2O_2-induced cytotoxicity in NGF-differentiated PC12 cells. Neurochem Res 43:1–15

Jin YC et al (2015) Intranasal delivery of RGD motif-containing osteopontin icosamer confers neuroprotection in the postischemic brain via α v β 3 integrin binding. Mol Neurobiol 53(8):5652–5663

Justicia C, Gabriel C, Planas AM (2000) Activation of the JAK/STAT pathway following transient focal cerebral ischemia: signaling through Jak1 and Stat3 in astrocytes. Glia 30:253–270

Kerrisk ME, Koleske AJ (2013) Arg kinase signaling in dendrite and synapse stabilization pathways: memory, cocaine sensitivity, and stress. Int J Biochem Cell Biol 45:2496–2500. https://doi.org/10.1016/j.biocel.2013.07.018

Krady JK, Basu A, Levison SW, Milner RJ (2002) Differential expression of protein tyrosine kinase genes during microglial activation. Glia 40:11

Kramar EA, Bernard JA, Gall CM, Lynch G (2003) Integrins modulate fast excitatory transmission at hippocampal synapses. J Biol Chem 278:10722–10730. https://doi.org/10.1074/jbc.M210225200

Li C et al (2014) Cytotoxicity of ultrafine monodispersed nanoceria on human gastric cancer cells. J Biomed Nanotechnol 10:1231

Liddelow SA et al (2017) Neurotoxic reactive astrocytes are induced by activated microglia. Nature 541:481

Liu J et al (2016) High glucose regulates LN expression in human liver sinusoidal endothelial cells through ROS/integrin αvβ3 pathway. Environ Toxicol Pharmacol 42:231

Mazalouskas M, Jessen T, Varney S, Sutcliffe JS, Veenstravanderweele J Jr, Cook EH Jr, Carneiro AM (2015) Integrin β3 haploinsufficiency modulates serotonin transport and antidepressant-sensitive behavior in mice. Neuropsychopharmacology 40:2015 **Official Publication of the American College of Neuropsychopharmacology**

Miranti CK, Leng L, Maschberger P, Brugge JS, Shattil SJ (1998) Identification of a novel integrin signaling pathway involving the kinase Syk and the guanine nucleotide exchange factor Vav1. Curr Biol 8:1289

Nishimura SL, Boylen KP, Einheber S, Milner TA, Ramos DM, Pytela R (1998) Synaptic and glial localization of the integrin alphav-beta8 in mouse and rat brain. Brain Res 791:271–282

Niu J, Azfer A, Rogers L, Wang X, Kolattukudy P (2007) Cardioprotective effects of cerium oxide nanoparticles in a transgenic murine model of cardiomyopathy. Cardiovasc Res 73:549–559. https://doi.org/10.1016/j.cardiores.2006.11.031

Patel A, Toia GV, Colletta K, Bradaric BD, Carvey PM, Hendey B (2011) An angiogenic inhibitor, cyclic RGDfV, attenuates MPTP-induced dopamine neuron toxicity. Exp Neurol 231:160

Pirmohamed T et al (2010) Nanoceria exhibit redox state-dependent catalase mimetic activity. Chem Commun (Camb) 46:2736–2738. https://doi.org/10.1039/b922024k

Planas AM, Soriano MA, Berruezo M, Justicia C, Estrada A, Pitarch S, Ferrer I (1996) Induction of Stat3, a signal transducer and transcription factor, in reactive microglia following transient focal cerebral ischaemia. Eur J Neurosci 8:2612–2618

Pourkhalili N et al (2011) Biochemical and cellular evidence of the benefit of a combination of cerium oxide nanoparticles and selenium to diabetic rats. World J Diabetes 2:204–210. https://doi.org/10.4239/wjd.v2.i11.204

Pozo K, Cingolani LA, Bassani S, Laurent F, Passafaro M, Goda Y (2012) β3 integrin interacts directly with GluA2 AMPA receptor subunit and regulates AMPA receptor expression in hippocampal neurons. Proc Natl Acad Sci USA 109:1323

Robinson RD, Spanier JE, Zhang F, Chan S-W, Herman IP (2002) Visible thermal emission from sub-band-gap laser excited cerium dioxide particles. J Appl Phys 92:1936–1941. https://doi.org/10.1063/1.1494130

Schäbitz WR et al (2003) Neuroprotective effect of granulocyte colony-stimulating factor after focal cerebral ischemia. Stroke 34:745–751

Scheiffele P, Fan J, Choih J, Fetter R, Serafini T (2000) Neuroligin expressed in nonneuronal cells triggers presynaptic development in contacting axons. Cell 101:657–669

Schubert D, Dargusch R, Raitano J, Chan SW (2006) Cerium and yttrium oxide nanoparticles are neuroprotective. Biochem Biophys Res Commun 342:86–91. https://doi.org/10.1016/j.bbrc.2006.01.129

Suzuki S, Tanaka K, Nogawa S, Dembo T, Kosakai A, Fukuuchi Y (2001) Phosphorylation of signal transducer and activator of transcription-3 (Stat3) after focal cerebral ischemia in rats. Exp Neurol 170:63–71

Takeuchi Y, Suzawa M, Kikuchi T, Nishida E, Fujita T, Matsumoto T (1997) Differentiation and transforming growth factor-beta receptor down-regulation by collagen-α2β1 integrin interaction is mediated by focal adhesion kinase and its downstream signals in murine osteoblastic cells. J Biol Chem 272:29309

Thameem Dheen S, Kaur C, Ling EA (2007) Microglial activation and its implications in the brain diseases. Curr Med Chem 14:1189–1197

Tuttolomondo A, Pecoraro R, Pinto A (2014) Studies of selective TNF inhibitors in the treatment of brain injury from stroke and trauma: a review of the evidence to date. Drug Des Dev Ther 8:2221

Visavadiya NP et al (2016) Integrin-FAK signaling rapidly and potently promotes mitochondrial function through STAT3. Cell Commun Signal 14:32

Wang Y et al (2016) Optimization of RGD-containing cyclic peptides against αγβ3 integrin. Mol Cancer Ther 15:232–240. https://doi.org/10.1158/1535-7163.MCT-15-0544

Wu H, Chen H, Sun Y, Wan Y, Wang F, Jia B, Su X (2013) Imaging integrin α(v)β(3) positive glioma with a novel RGD dimer probe and the impact of antiangiogenic agent (Endostar) on its tumor uptake. Cancer Lett 335:75–80

Xiao W et al (2010) The use of one-bead one-compound combinatorial library technology to discover high-affinity αγβ3 integrin and cancer targeting arginine-glycine-aspartic acid ligands with a built-in handle. Mol Cancer Ther 9:2714–2723. https://doi.org/10.1158/1535-7163.MCT-10-0308

Xu CS, Wang ZF, Huang XD, Dai LM, Cao CJ, Li ZQ (2015) Involvement of ROS-alpha v beta 3 integrin-FAK/Pyk2 in the inhibitory effect of melatonin on U251 glioma cell migration and invasion under hypoxia. J Transl Med 13:1–11

Yasuda J, Okada M, Yamawaki H (2017) T3 peptide, an active fragment of tumstatin, inhibits H2O2-induced apoptosis in H9c2 cardiomyoblasts. Eur J Pharmacol 807:64–70

Zhang T et al (2018) Combination therapy with LXW7 and ceria nanoparticles protects against acute cerebral ischemia/reperfusion injury in rats. Curr Med Sci 38:144–152. https://doi.org/10.1007/s11596-018-1858-5